

**Realizing fast polysulfides conversion within yolk-shelled
NiO@HCSs nanoreactor as cathode host for high-performance
lithium-sulfur batteries**

Yujie Wu ^a, Dong Li ^a, Junda Pan ^a, Yajie Sun ^a, Wenzhi Huang ^a, Ming Wu ^a,
Bingkai Zhang ^a, Feng Pan ^b, Kaixiang Shi ^{a,*}, Quanbing Liu ^{a,*}

^a Guangzhou Key Laboratory of Clean Transportation Energy Chemistry, Guangdong Provincial Key Laboratory of Plant Resources Biorefinery, School of Chemical Engineering and Light Industry, Guangdong University of Technology, Guangzhou 510006, PR China.

^b School of Advanced Materials, Peking University Shenzhen Graduate School, Shenzhen 518055, PR China.

* Corresponding author. E-mail address: shikx@hotmail.com (K. Shi), liuqb@gdut.edu.cn (Q. Liu)

Experimental Section

Chemicals. All chemicals are purchased from Macklin Company, including dopamine hydrochloride ($C_8H_{11}NO_2 \star HCl$), tetraethyl orthosilicate (TEOS), ammonia solution (25%–28%), urea (CH_4N_2O), nickel nitrate ($Ni(NO_3)_2 \star 6H_2O$), sublimed sulfur (S), sodium hydroxide (NaOH) and ethanol (C_2H_6O). All chemicals do not require further purification.

Synthesis of hollow carbon spheres (HCSs). 1 mL ammonia solution was added into the mixture containing water (80 mL) and ethanol (24 mL), and stirring for 30 min to form homogeneous solution A. Then adding 1 mL TEOS to solution A and stirring vigorously at room temperature. Subsequently, the solution B that 0.4 g DA dissolving 9 mL deionized water was poured into the above mixture. After continuous reaction for 24 hours, the $SiO_2@PDA$ product was accumulated by centrifuging the above solution with methanol and water and then dried at $60^\circ C$ for 12 h. The $SiO_2@HCSs$ were obtained by heating at $800^\circ C$ for 2 hours with $2^\circ C \text{ min}^{-1}$ under nitrogen atmosphere. After that, the black powder was etched in 3M NaOH solution at room temperature for 24 h to remove SiO_2 and gain HCSs.

Synthesis of yolk-shelled $NiO@HCSs$. To synthesize the yolk-shelled $NiO@HCSs$, a simple hydrothermal method was used. First of all, adding 20 mg $SiO_2@C$ to 35 mL deionized water with ultrasound for 30 min, then 300 mg urea and 60 mg $Ni(NO_3)_2 \star 6H_2O$ were separately dissolved above solution for stirring 1 hour, dispersed evenly and transferred the mixture to Teflon-lined stainless steel autoclave (100 mL) and kept at $120^\circ C$ for 16 h. After that, the $Ni(OH)_2@HCSs$ was collected by washing with deionized water and methanol and then dried at $60^\circ C$ overnight. Finally the YS $Ni(OH)_2@HCSs$ was calcinated at $350^\circ C$ for 2 hours at the heating rate of $2^\circ C \text{ min}^{-1}$ under nitrogen atmosphere to obtain YS $NiO@HCSs$.

Preparation of the S/YS $NiO@HCSs$ cathode. The S/YS $NiO@HCSs$ composite was prepared by the melt-diffusion method. Typically, the YS $NiO@HCSs$ and sublimed sulfur were ground with a weight ratio of 1:3 in an agate mortar for 30 min, followed by heating at $155^\circ C$ for 12 h. The S/HCSs was prepared with the same method.

Visualized adsorption test. 0.5mmol L⁻¹ Li₂S₆ solution was prepared by sulfur and Li₂S powders (the molar ratio is 5:1) in the dimethoxyethane (DME) and dioxolane (DOL) (v/v =1:1) mixed solution with vigorous stirring at 60°C for 12h. 20mg HCSs, NiO@HCSs samples were added to 2 mL above solutions, respectively. After leaving for 6 hours, the color changes of solution were observed and tested the ex-situ ultraviolet-visible (UV) absorption spectra.

Polysulfide conversion kinetic test. The electrodes were prepared by mixing samples, Ketjen black, and PVDF with a weight ratio of 8:1:1 in NMP solvent, and the slurry was coated onto Al foil. 0.5 mol L⁻¹ Li₂S₆ electrolyte was prepared by stirring S₈ and Li₂S in the electrolyte with 1 M LiTFSI in DOL/DME (v/v =1:1) at 60°C. Two identical electrodes were used as the working and the counter electrodes with 20mL Li₂S₆ solution as electrolyte. The CV measurements of the symmetric cells were measured between -1~1 V at a scan rate of 5 mV s⁻¹.

Li₂S nucleation measurements. 0.5 mol L⁻¹ Li₂S₈ solution was prepared by sulfur and Li₂S powders (the molar ratio is 7:1) in the DME and DOL (v/v =1:1) mixed solution with 1.0 M LiTFSI. The cathodes were carbon paper (CP) containing 5 mg samples, and the lithium metal acted as the counter electrode and reference electrode. The batteries were discharged galvanostatically at 0.112 mA to 2.06 V and kept potentiostatically at 2.05 V for Li₂S to nucleate.

Li₂S dissolution and S₈ transformation test. For dissolution of Li₂S, the assembled above cells were first discharged to 1.80V at 0.134mA galvanostatically followed by discharge at 1.80 V under 0.134 mA for complete transformation of LiPSs into solid Li₂S. Then, they were charged at 2.40 V potentiostatically for the oxidization process from solid Li₂S to soluble LiPSs. For the transformation of S₈, the cells were directly potentiostatic discharge at 2.2 V for 50000s.

Materials characterization. The morphologies were investigated by scanning electron microscopy (SEM) (JSM-6700, JEOL, Japan). The inner structure and element dispersion were tested by Transmission electron microscope (TEM) and energy dispersive X-ray spectroscopy (EDS), respectively (Titan G260-300). Crystal structures were characterized by X-ray diffraction (XRD) using Cu-K α radiation.

The surface chemistry was analyzed by XPS spectra using Thermo Scientific™ K-Alpha™ spectrometer equipped with a monochromatic Al K α . The pore size distribution and specific surface area were obtained from nitrogen adsorption and desorption experiments (Micromeritics TriStar II). The sulfur content in hosts was conducted by TGA measure at a heating rate of 5°C min⁻¹ under N₂ atmosphere (NETZSCH TG 209 F3). Raman spectra were performed on a LabRAM HR800 (Horiba).

Electrochemical measurements. First of all, the hosts were mixed with Ketjen black (KB) and PVDF in a weight ratio of 8:1:1 in NMP to obtain slurry. The slurry was coated on Al foil, dried at 60 °C overnight and cut into 13 mm disks in diameter where the sulfur loading was about 1-1.2 mg cm⁻² and E/S=15 uL mg⁻¹. The lithium metal and Celgard 2400 acted as anode and a separator, respectively. DOL and DME (v/v = 1:1) mixed solution with 1 wt.% LiNO₃ additive and 1.0 M LiTFSI was used as the electrolyte. The galvanostatic discharge-charge test was conducted by a Neware system with a voltage of 1.7~2.8 V. The CV curves and EIS were tested by Autolab electrochemical workstation.

Theoretical Calculations. All calculations were performed based on the density functional theory (DFT) method under periodic boundary conditions, in complement with the Vienna Ab-initio Simulation Package (VASP). The projector augmented wave (PAW) method with a generalized gradient approximation based on the Perdew-Burke-Erzerhof (PBE) exchange correlation functional are adopted. Integration in the Brillouin zone was performed on the basis of the Monkhorst-Pack scheme using a Γ centered $3 \times 3 \times 1$ K-point mesh in each primitive lattice vector of the reciprocal space for optimization. The convergence criterion for the electronic structure iteration was set to be 10⁻⁵ eV, and that for geometry optimization was set to be 0.02 eV Å⁻¹ on force. The plane-wave cutoff energy of 400 eV was used, and the model were built in a unit cell along a and b directions with a vacuum region of up to 20 Å along the c directions avoids the interaction between adjacent layers. Lattice parameter and internal atomic positions were fully optimized.

YS NiO@HCSs and HCSs structures were chosen to investigate their interactions with LiPSs molecules (Li_2S_2 , Li_2S_4 , Li_2S_6). The adsorption energy (E_{bind}) was calculated according to the following equation:

$$E_{\text{bind}} = E_{\text{product}} - E_{\text{surface}} - E_{\text{molecular}} \quad (1)$$

where $E_{\text{molecular}}$, E_{surface} , and E_{product} are characterized as the complete energies of LiPSs molecules (Li_2S_2 , Li_2S_4 , Li_2S_6), NiO (200) or carbon surface, and the adsorbed products, individually.

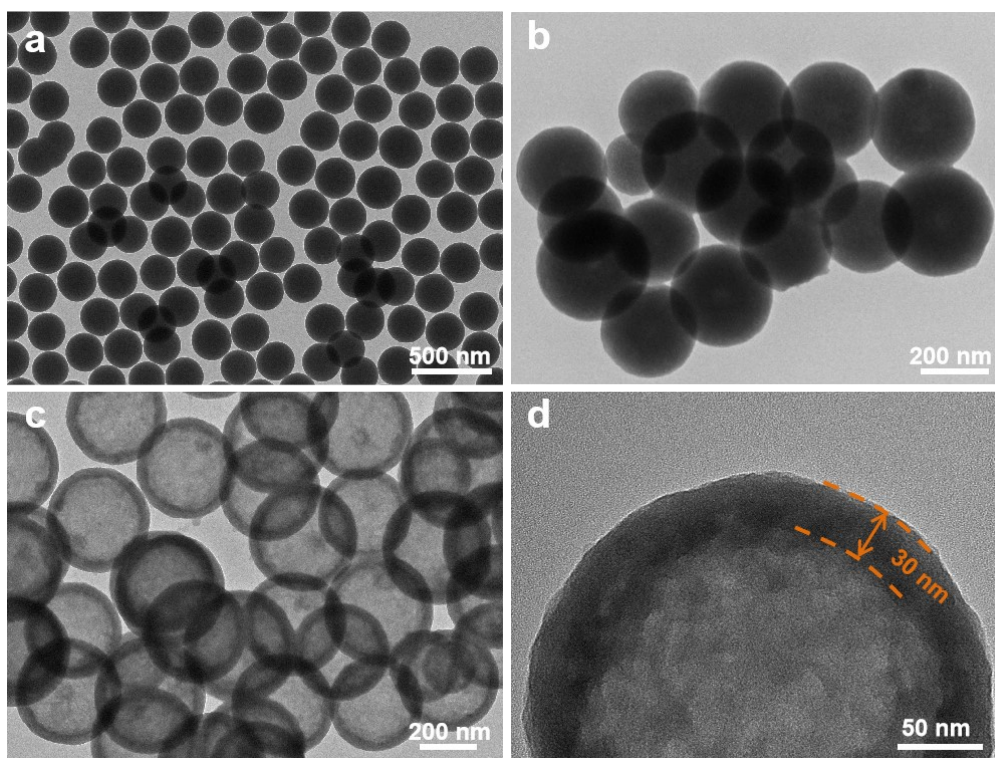


Figure S1. TEM image of (a) SiO₂, (b) SiO₂@C and (c, d) HCSs.

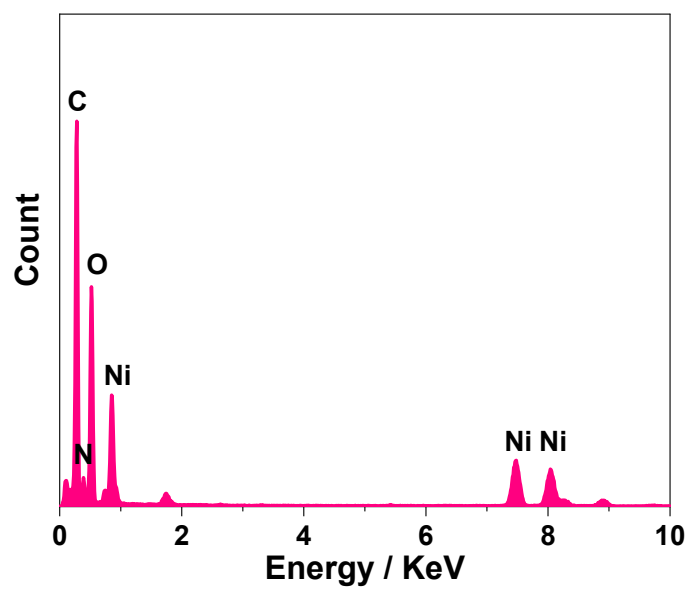


Figure S2. EDX spectrum of YS NiO@HCSs.

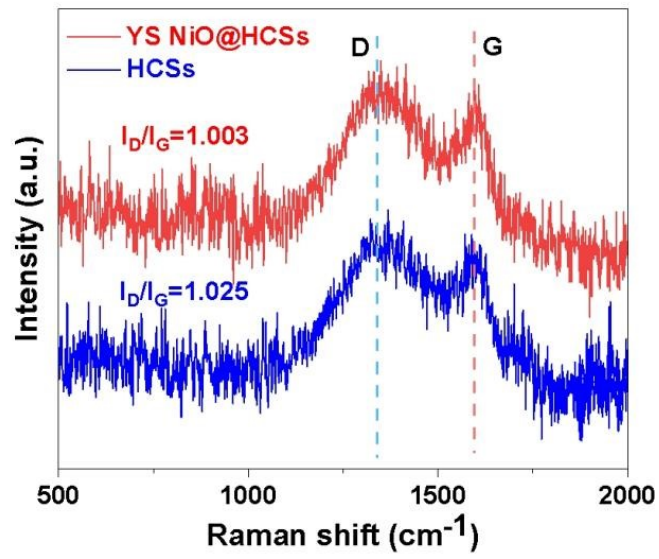


Figure S3. Raman spectra of the samples.

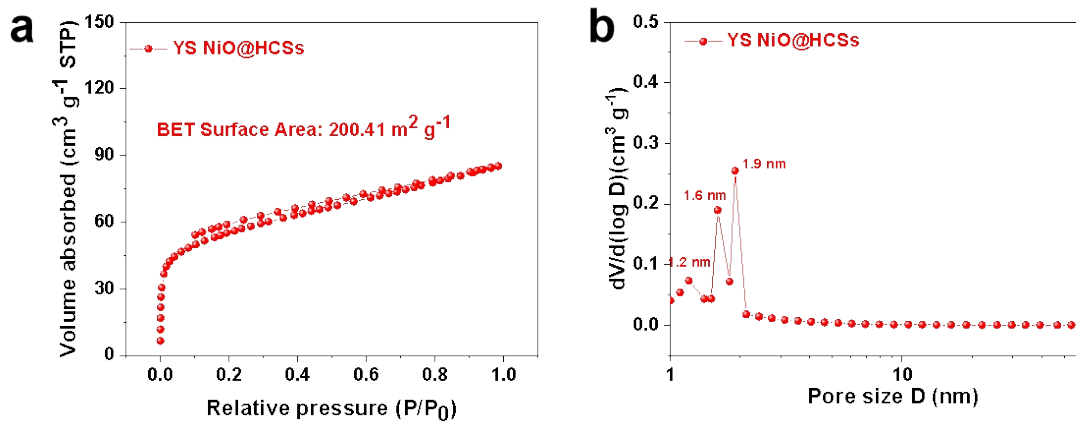


Figure S4. Nitrogen adsorption–desorption isotherms and pore size distribution of of YS NiO@HCSs, respectively.

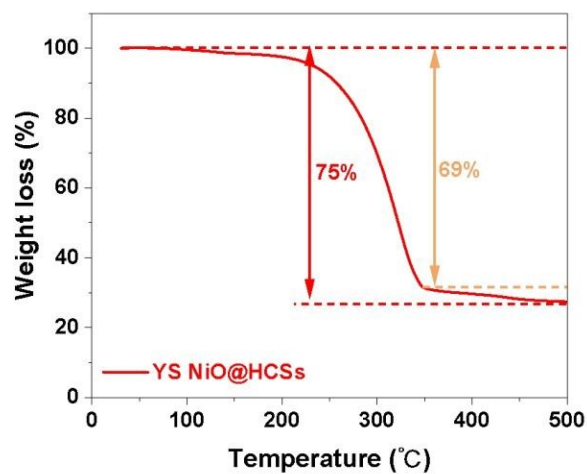


Figure S5. TGA curves of S/YS NiO@HCSs.

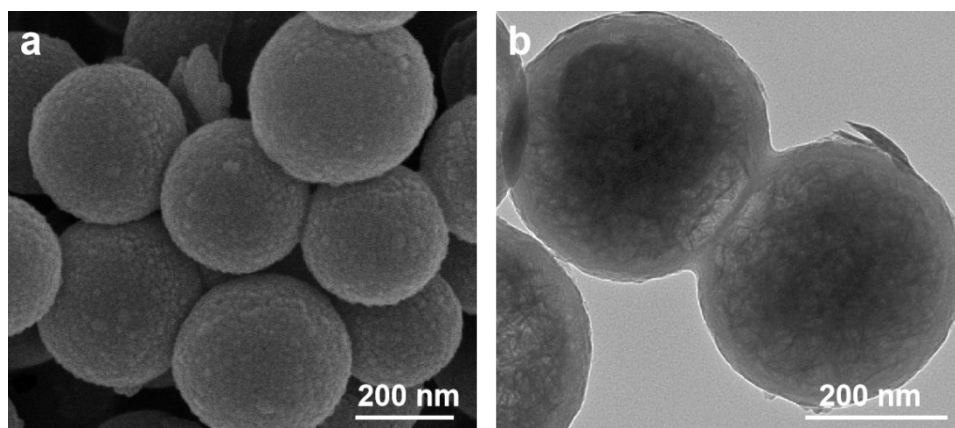


Figure S6. SEM and TEM of S/YS NiO@HCSs.

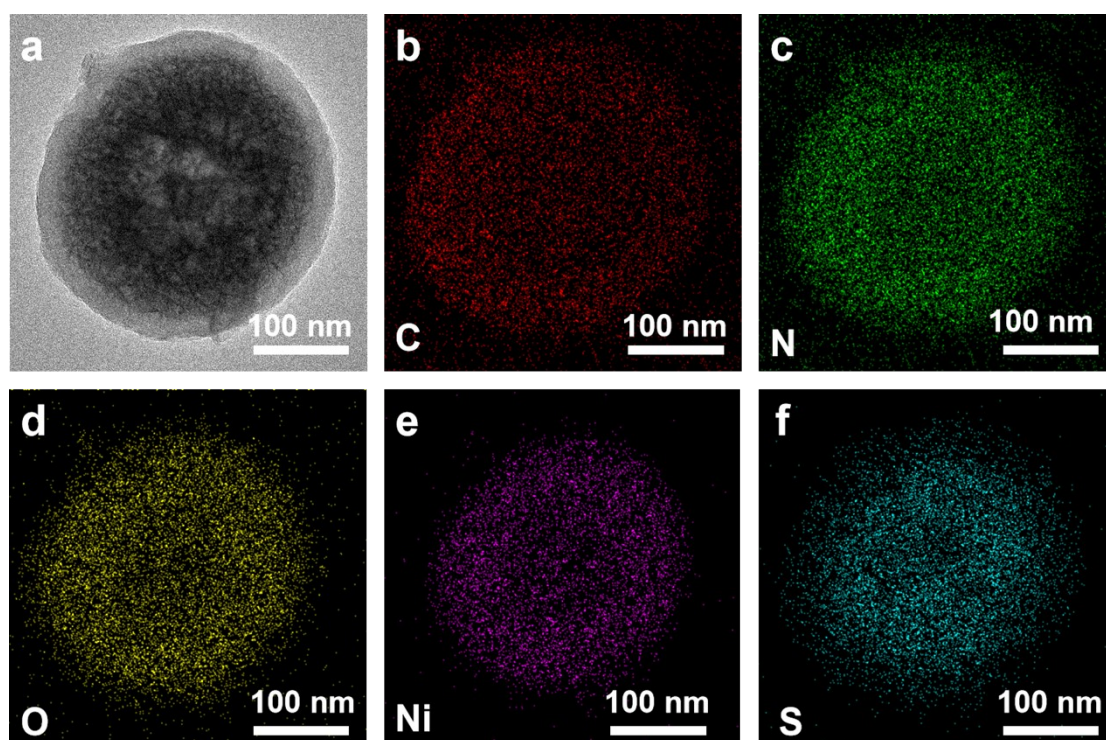


Figure S7. TEM morphology of S/YS NiO@HCSs and the corresponding elemental mapping images of C, N, O, Ni and S.

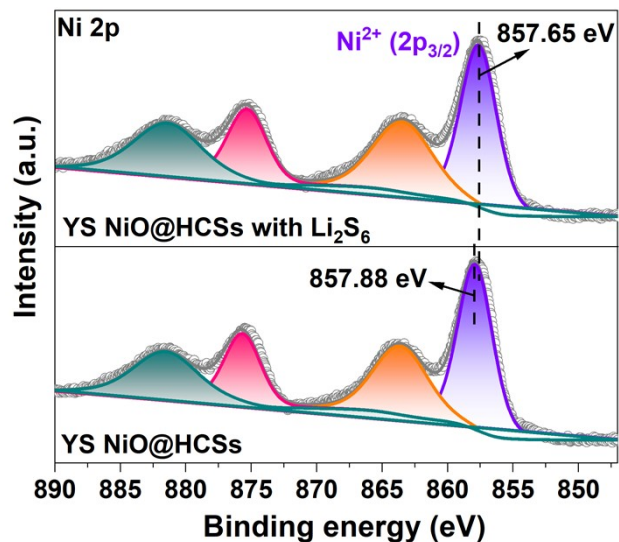


Figure S8. Ni 2p XPS spectra of YS NiO@HCSs with and without LiPS adsorption.

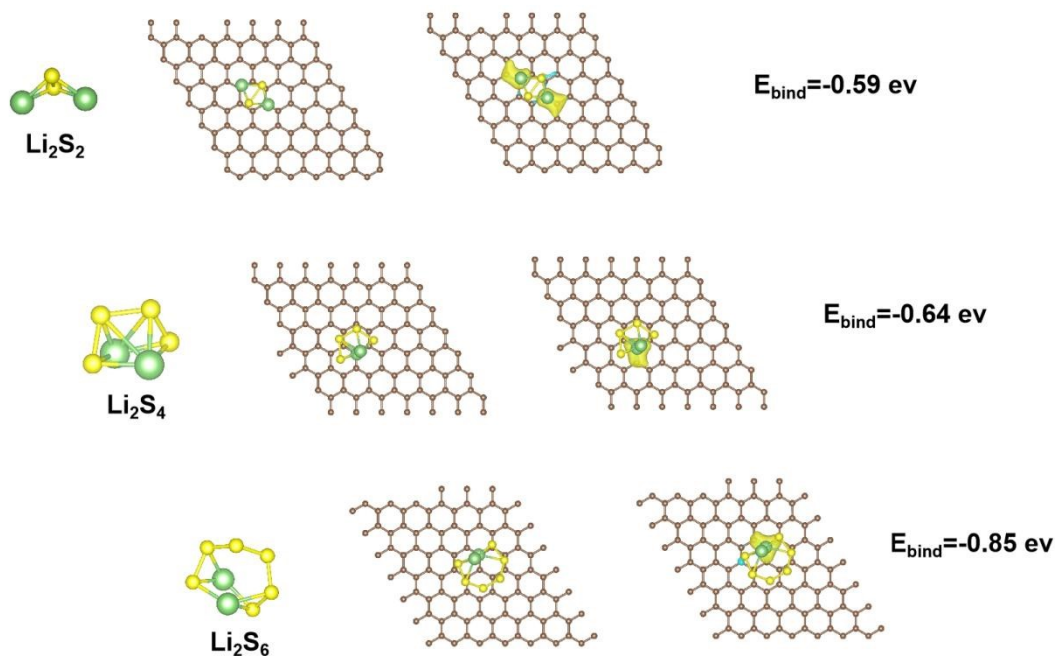


Figure S9. DFT-calculated molecular structures of Li_2S_n ($n=2, 4, 6$), optimized structures, electronic differential density of carbon surface binding with Li_2S_n .

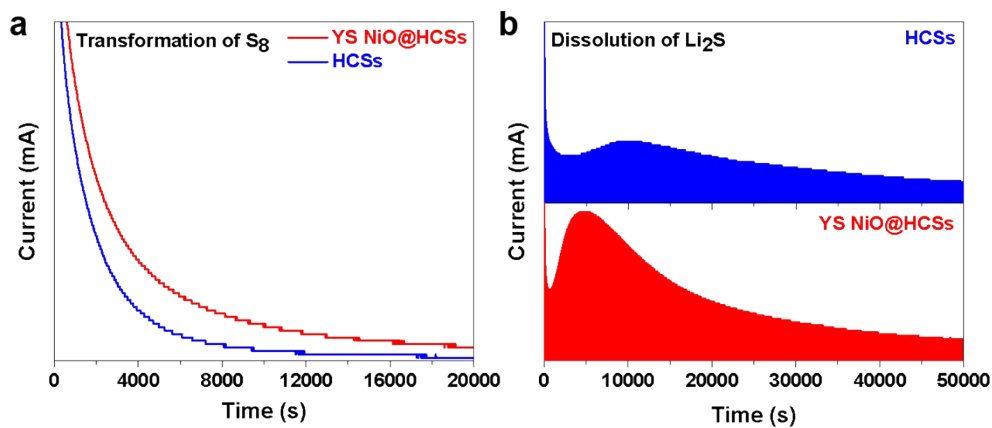


Figure S10. (a) Transformation profiles of S₈ and (b) Dissolution profiles of Li₂S with YS NiO@HCSs and HCSs.

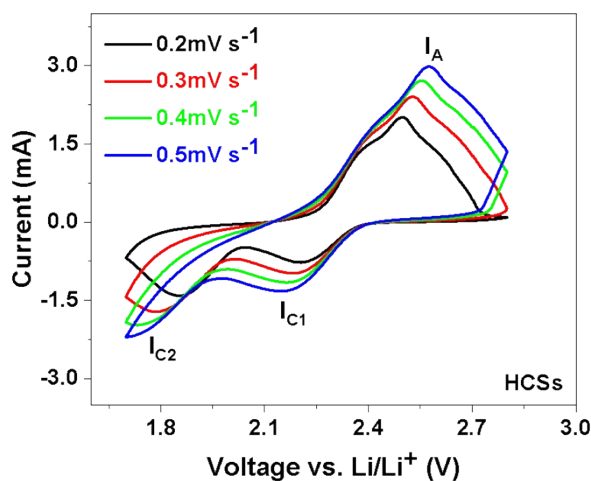


Figure S11. CV curves at various scanning speed of HCSs.

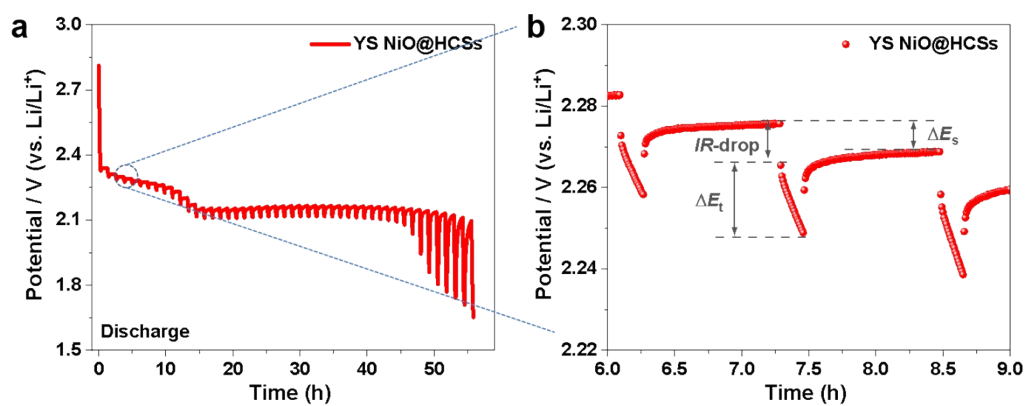


Figure S12. (a) The GITT curves and (b) the parameters calculate D_{Li^+} of S/YS NiO@HCSs.

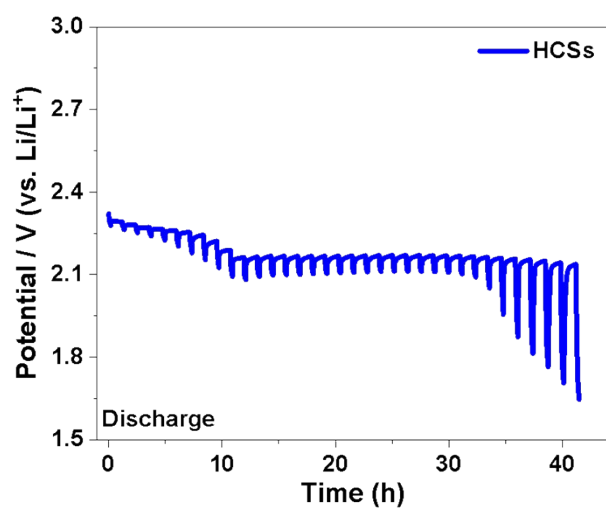


Figure S13. The GITT curves of S/HCSs.

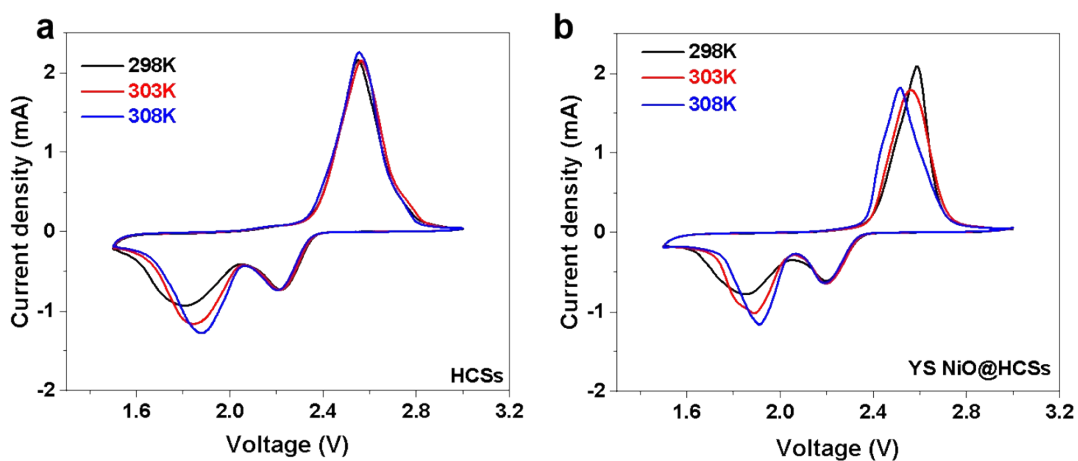


Figure S14. CV curves of the Li-S batteries using (a) YS NiO@HCSs, and (b) HCSs as catalysts at various temperatures.

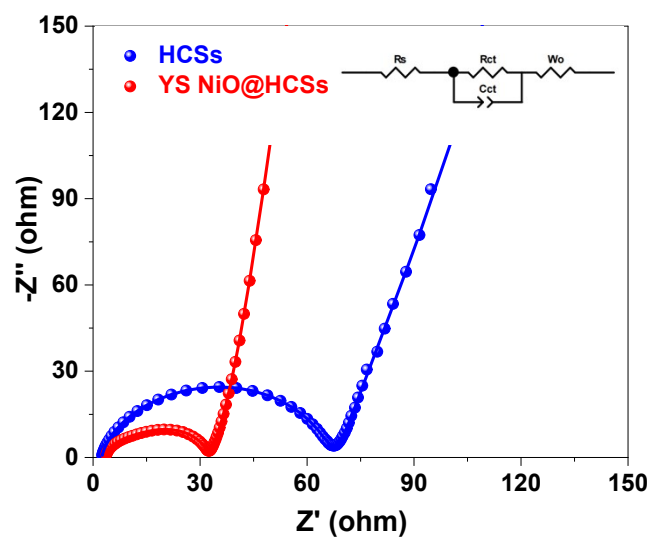


Figure S15. The EIS of fresh batteries with different cathodes.

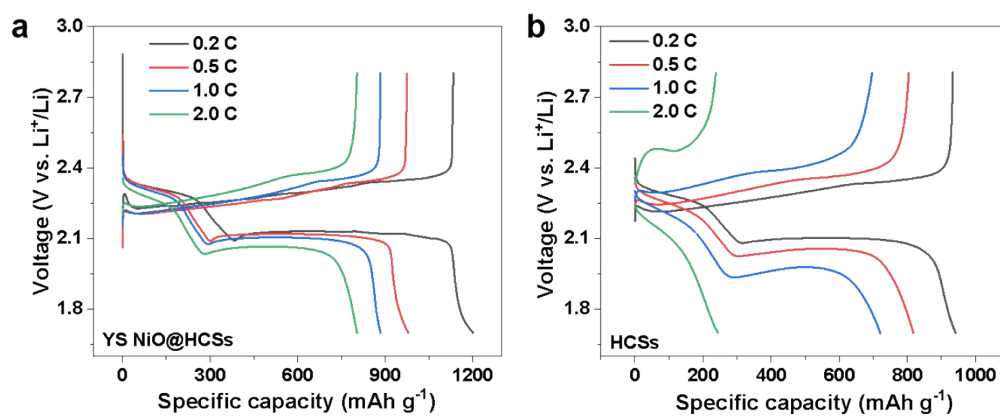


Figure S16. Galvanostatic discharge-charge curves at various current densities with S loading of $1.0\text{-}1.2\text{ mg cm}^{-2}$ of (a) YS NiO@HCSs and (b) HCSs.

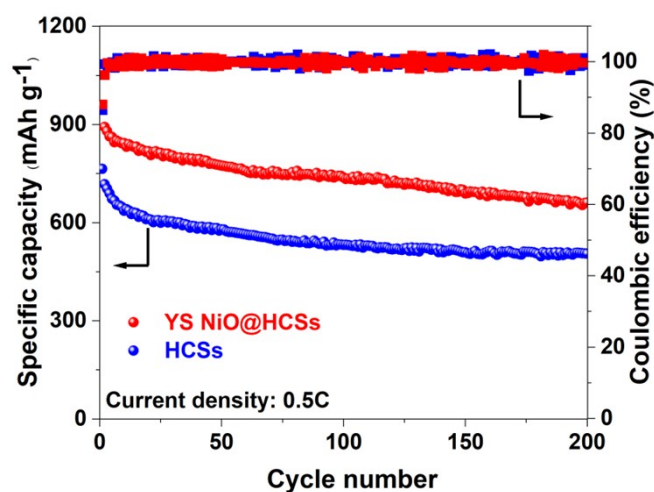


Figure S17. Cyclic stability performance at 0.5 C.

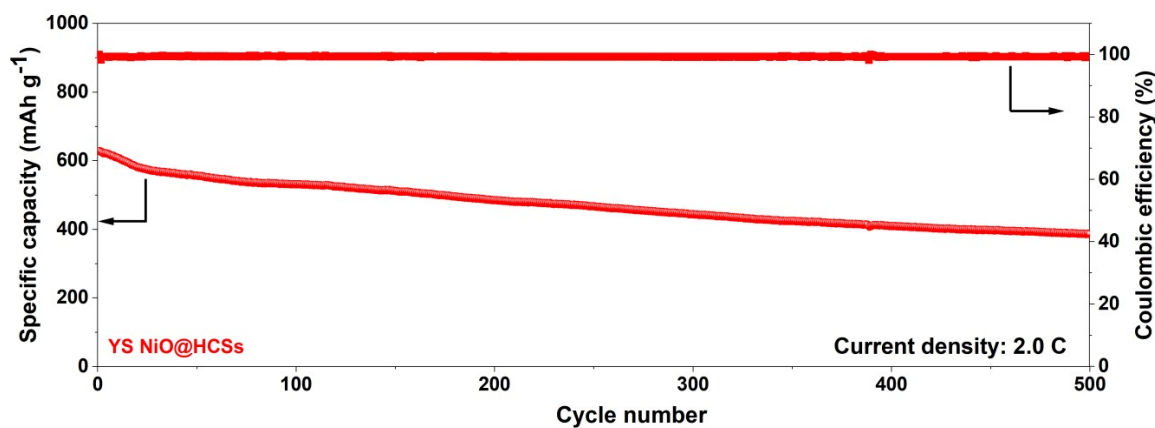


Figure S18. Cyclic stability performance at 2.0 C.

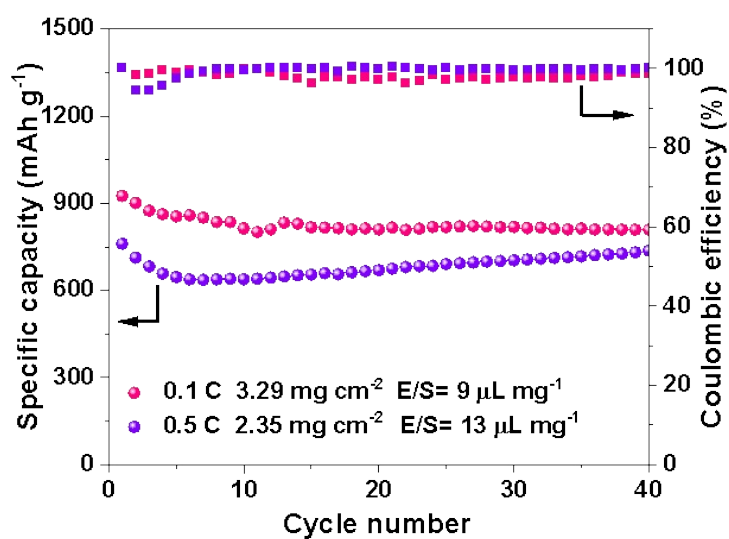


Figure S19. Cyclic stability performance with higher sulfur loadings of YS NiO@HCSs at 0.1 C and 0.5 C.

Table S1. Comparison of electrochemical performance between YS NiO@HCSs and other sulfur host material reported by previous literatures.

Sample	Sulfur content (wt.%)	Areal mass (mg cm ⁻²)	Rate (C)	Cycle number	specific capacity (mAh g ⁻¹)	Reference
YS NiO@HCSs	75	1-1.2	1	300th	568	This work
CoP@HPCN-MWCNT	70	1.1	0.2	300th	630	[1]
Fe/Fe ₃ C-MWCNTs@ACT	62.3	1.5	1	627th	451	[2]
SMC-8	70.1	0.8-1.1	0.2	400th	626	[3]
YS-C	70	0.56	0.5	200th	686	[4]
Co@NCNT	76	1.3	1	500th	428	[5]
Co-Zn/Zn-C-800	50	1.3	1	500th	590	[6]
CoSe ₂ /C	73	1.2-1.5	1	400th	503	[7]
CoS ₂ @NC/MWCNT-800	61.6	1	1	300th	496	[8]
CNTs-VSe ₂ -VO _x	70.3	1.5	0.5	100th	788.1	[9]
Co/N-PCNs	68	0.8-1.0	1	200th	633	[10]
CoFe ₂ O ₄ @C	74.3	1	0.5	100th	821	[11]
MoSe ₂ @MCHS	/	1	0.2	150th	703	[12]
MoSe ₂ /N-rGO	62	1.1	0.2	100th	692	[13]
Fe-Ni-P@NC	69	1	1	500th	470	[14]
AZT-C	70	1	0.5	290th	555	[15]

References

- [1] Z. Ye, Y. Jiang, J. Qian, W. Li, T. Feng, L. Li, F. Wu, R. Chen, *Nano Energy*, 2019, 64, 103965.
- [2] R. Chen, Y. Zhou, X. Li, *Nano Lett.*, 2022, 22, 1217-1224.
- [3] Y. Liu, M. Chen, M. Hu, Y. f. Gao, Y. Zhang, D. Long, *Chem. Eng. J.*, 2021, 406, 126781.
- [4] G. D. Park, D. S. Jung, J.-K. Lee, Y. C. Kang, *Chem. Eng. J.*, 2019, 373, 382-392.
- [5] A. H. Shao, Z. Zhang, D. G. Xiong, J. Yu, J. X. Cai, Z. Y. Yang, *ACS Appl. Mater. Inter.*, 2020, 12, 5968-5978.
- [6] M. Yang, X. Wang, J. Wu, Y. Tian, X. Huang, P. Liu, X. Li, X. Li, X. Liu, H. Li, *J. Mater. Chem. A*, 2021, 9, 18477-18487.
- [7] X. Sun, S. Zeng, R. Man, L. Wang, B. Zhang, F. Tian, Y. Qian, L. Xu, *Nanoscale*, 2021, 13, 10385-10392.
- [8] C.-H. Chen, S.-H. Lin, Y.-J. Wu, J.-T. Su, C.-C. Cheng, P.-Y. Cheng, Y.-C. Ting, S.-Y. Lu, *Chem. Eng. J.*, 2022, 431, 133924.
- [9] J. Qi, T. Wu, M. Xu, Z. Xiao, *ACS Appl. Mater. Inter.*, 2021, 13, 39186-39194.
- [10] S. Liu, J. Li, X. Yan, Q. Su, Y. Lu, J. Qiu, Z. Wang, X. Lin, J. Huang, R. Liu, B. Zheng, L. Chen, R. Fu, D. Wu, *Adv. Mater.*, 2018, 30, 1706895.
- [11] L.-L. Gu, J. Gao, C. Wang, S.-Y. Qiu, K.-X. Wang, X.-T. Gao, K.-N. Sun, P.-J. Zuo, X.-D. Zhu, *J. Mater. Chem. A*, 2020, 8, 20604-20611.
- [12] L. Meng, Y. Yao, J. Liu, Z. Wang, D. Qian, L. Zheng, B.-L. Su, H.-E. Wang, *J. Energy Chem.*, 2020, 47, 241-247.
- [13] H. Wong, X. Ou, M. Zhuang, Z. Liu, M. D. Hossain, Y. Cai, H. Liu, H. Lee, C. Z. Wang, Z. Luo, *ACS Appl. Mater. Inter.*, 2019, 11, 19986-19993.
- [14] C. Song, Q. Jin, W. Zhang, C. Hu, Z. Bakenov, Y. Zhao, *J. Colloid Interf. Sci.*, 2021, 595, 51-58.
- [15] D. Kyom Kim, J. Seul Byun, S. Moon, J. Choi, J. Ha Chang, J. Suk, *Chem. Eng. J.*, 2022, 441, 135945.